

Geomorphological and geomorphometrical characterization of subglacial channels on Devon Island, Nunavut, Canada

Simona F. Ruso^{1,2}, Anna Grau Galofre³, Gordon R. Osinski¹

¹Department of Earth Sciences, University of Western Ontario, London, N6A 3K7, Canada

²Institute for Earth and Space Exploration, London, N6A 3K7, Canada

³Laboratoire de Planétologie et Géosciences, Nantes, 44322, France

Correspondence to: Simona F. Ruso (sruso@uwo.ca)

Abstract. Subglacial channels are morphologically and morphometrically distinct in comparison to fluvial channels, yet their identification from remote sensing data is still problematic. To contribute to the current set of criteria used to identify such channels, we performed detailed field observations of two subglacial channel networks on Devon Island, Nunavut, Canada. In planform, these channels are isolated, finger-like networks that drain into a main stem and have distinct cross-sectional and longitudinal profiles. Cross-sections are flat-bottomed with steep walls and longitudinal profiles are convex and exhibit undulations, typical of pressurized water flow (i.e., subglacial flow). To facilitate remote sensing identification, we interrogated how well-known scaling relationships capturing hydraulics and mass balance dynamics of fluvial systems differ in subglacial channels. Scaling relationships typically used to discern connections between discharge and channel and catchment size in fluvial systems were applied to both networks, yielding trends distinct from the fluvial literature. We suggest that the weakly correlated relationship we found between channel discharge and the size of the drainage area indicates a discrete point or line source of water, such as a moulin or crevasse.

1 Introduction

1.1 Glacial landscapes and subglacial channels

The distribution of glacial landforms and landform assemblages is a useful tool in reconstructing the extent, thickness, margin location, flow direction, thermal regime, and dynamics of former ice sheets (Boulton, 1972; Clayton and Moran, 1974; Clark et al., 2018; Dewald et al., 2022; Kleman, 1992; Glasser and Bennett, 2004; Cuffey and Paterson, 2010). Glacial landform assemblages reflect the basal thermal state of the ice: cold (frozen), warm-based (basal meltwater), or polythermal (seasonal or localized basal meltwater) (O Cofaigh et al., 1999). Under warm-based ice sheets, glacial flow dominated by ice sliding over the substrate produces distinctive landforms, which include erosional forms such as striations, grooves, polished bedrock, roches moutonnées, and terminal glacial valleys and fjords (Kleman and Borgström, 1996). Depositional landforms associated with glacial sliding include terminal moraine ridges and massive tillite deposits. Deformational features related to glacial sliding on soft sediment include, from lesser to larger basal shear, ribbed moraines, circular and elongated forms, drumlins, and megascale glacial lineations (Vérité et al., 2023, 2022).



In contrast to warm-based glaciers, cold-based glaciers are frozen to the bed and move only by internal deformation, protecting the underlying landscape and preserving features such as vegetation and patterned ground (Atkins, 2013; Sugden et al., 1991). While lacking the sheet-like basal meltwater that induces sliding of warm-based ice, some studies have documented evidence of active subglacial processes occurring in cold-based glaciers such as minimal sliding, entrainment, and sediment deformation (e.g., Atkins, 2013; Cuffey et al., 2000; Fitzsimons et al., 2001; Hambrey & Fitzsimons, 2010). The presence of lateral meltwater channels is typically the main indicator of cold-based glaciation; these channels form as supraglacial meltwater flows to the glacier margins and incises into the bedrock adjacent to the glacier, forming a series of short, parallel channels (Kleman and Borgström, 1996; O Cofaigh et al., 1999; Atkins and Dickinson, 2007).

Polythermal-based glaciation can record a variety of glacial landforms indicative of both warm- and cold-based regimes. Areas of warmer ice display evidence of meltwater accumulation and sliding, whereas under colder parts of the ice minimal erosion and preservation of underlying landforms is expected. However, understanding the distribution of cold- and warm-based ice within a polythermal system can be challenging with overriding and subsequent modification of the landscape during deglaciation. Kleman et al., (1999) used landform assemblages to discuss three types of thermal zonation around a migrating warm-based zone: either via up-glacier migration from the ice margin, patchy up-glacier migration controlled by areas of high topography that remain cold-based, or fast-flowing ice streams that concentrate basal sliding in a laterally constrained zone over short periods of time. More recently, Vérité et al., (2024) described ice-meltwater-bed interactions of ice sheets based on the evolution of subglacial landforms in response to variations in ice flow velocities. These potentially complex systems can assist in understanding the evolution of the ice sheet, as well as in linking landform assemblages to episodes of advance or retreat based on superimposing relationships.

The distribution of subglacial meltwater routes in Fennoscandia illustrate that glacial landscapes are composite records of glaciation (Greenwood et al., 2016), and, at the ice sheet-scale, meltwater drainage (and derived landforms) may be influenced by topography created by previous glaciations (Dewald et al., 2022; Simkins et al., 2021). At the ice sheet-scale, Dewald et al. (2022) defined “subglacial meltwater routes,” a term that collectively describes subglacial meltwater landforms, including eskers (depositional), glaciofluvial hummocky corridors, tunnel valleys (erosional), and subglacial meltwater channels (erosional). In the Fennoscandian Ice Sheet there was an association between a decrease in subglacial meltwater route density and proximity to a paleo-ice divide, as well as absence of meltwater routes in areas that have been interpreted as cold-based (Dewald et al., 2022). Subglacial meltwater route presence can, therefore, be a useful indicator of the transition from warm- to cold-based zones of an extinct ice sheet, whereas their direction follows that of former ice flow. Meltwater drainage routes formed beneath warm- to polythermal-based ice sheets are useful in reconstructing flow patterns and can provide important insight into meltwater generation and drainage, and glacial sliding dynamics under former ice sheets (Kleman & Borgström, 1996; Glasser & Bennett, 2004; Storrar et al., 2014).

This study focusses on the morphology and comparative morphometry of subglacial meltwater channels within the ice sheet drainage system. Subglacial channels are conduits that either incise upward into overlying ice (‘R-channels’, Rothlisberger, 1972), down into soft, cohesionless sediment (‘canals’, Walder and Fowler, 1994), or down into bedrock (‘N-channels’, Nye,



1976). Channel type nomenclature is based on their position relative to the glacier or, in the case of relict features, based on characteristics such as sinuosity, dimension, and planform morphology (Table 1) (Greenwood et al., 2007).

Table 1. Morphological characteristics of meltwater channels. Modified from Greenwood et al. (2007).

Characteristic	Subglacial	Lateral	Proglacial	Supraglacial/Englacial
Longitudinal profile	Topographic undulations in longitudinal profile ^{1,2,3} Ungraded confluences ⁴	Gentle gradient ¹	Steep slopes ¹²	Low gradient ¹¹ Stepped ¹³
Cross section	Shallow, trapezoidal cross-sections ³	Flat-bottom, steep sides ¹¹	Wide and deep ¹⁰ Terraces ¹²	Approximately constant width ¹¹
Planform	Abrupt beginning and end ^{1,2} Complex bifurcating and anastomosing system ^{4,5}	Abrupt termination ¹⁰ Straight ¹¹	Occasional bifurcation ¹⁰	Sinuosity ¹¹
Sinuosity	Highly sinuous ⁵	Approximately straight ⁵	Meandering ¹⁰	Sinuosity ¹¹
Associated landforms	May be associated with eskers ⁶ Associated with other glacial landforms ⁷ Cavities and potholes may be present ⁴	Series of parallel channels ^{1,8,9} May be isolated from other glacial features ^{6,9} Located on valley sides ¹⁰	Crater chains ¹⁰	Crescentic valley forms on hill face ¹
Deviation from topography?	May deviate from topographic gradient ^{1,3,4}	Flow follows local topography ¹	Flow follows topography ¹¹	Flow follows ice topography/gradient
	¹ Sissons, (1961); ² Glasser and Smith, (1999); ³ Grau Galofre et al., (2018); ⁴ Sugden et al., (1991); ⁵ Clapperton, (1968); ⁶ Kleman and Borgström, (1996); ⁷ Dewald et al., (2022); ⁸ Schytt, (1956); ⁹ Dyke, (1993); ¹⁰ Benn & Evans, (1998); ¹¹ (Price, 1960); ¹² Marren & Toomath, (2014); ¹³ Vatne and Irvine-Fynn, (2016)			

68 In cold- to polythermal-based glacial environments, subglacial, proglacial, and supraglacial/englacial meltwater channels can sometimes be observed in addition to lateral meltwater channels. Subglacial channel and tunnel valley orientation is typically parallel to the flow of the glacier, where supra- or englacial meltwater is carried to the bed and driven down-ice (Kehew et al., 2012). Subglacial channels have previously been identified based on their flat-bottomed cross-sections and undulating longitudinal profiles (Sugden et al., 1991; Greenwood et al., 2007). Additionally, subglacial meltwater channels such as those described by Sugden et al. (1991) and Lewis et al. (2006), among others, in the Antarctic Dry Valleys, exhibit complex topologies with interconnected or anastomosing patterns interpreted to indicate erosion by episodic, high-energy subglacial flows. Subglacial channels are typically metre-scale features, but tunnel valleys, typically incised in sedimentary rocks as opposed to harder substrates, can reach widths at the kilometre-scale. For example, Jørgensen & Sandersen (2006) describe



78 up to 3 km-wide composite tunnel valleys that formed during the Late Weichselian glaciation in Denmark ~25 - 10 ka BP
(Mangerud and Berglund, 1978).

80 **1.2 Study area: Devon Island**

82 **1.2.1 Geography and geology**

82 Devon Island is a 55,247 km² uninhabited island located at ~75° N / 87° W in the Canadian Arctic Archipelago. It is
dominated by an inland plateau region comprised of dolomite and limestone bedrock of the almost flat-lying Arctic Platform
84 sedimentary succession (Thorsteinsson and Mayr, 1987). Along the eastern and north-eastern coasts, exposures of
metamorphic and metasedimentary rocks of the Canadian Shield are observed (Osinski et al., 2005). Cliffs bound the island
86 to the north and south, where several large fjords incise into the plateau (Figs. 1, 2). Grinnell Peninsula, in western Devon
Island, is the lowest point of the plateau at around 300 m before gently sloping upward to a maximum elevation of 600 m
88 towards the east (Dyke, 1999). Eastern Devon Island is currently occupied by the Devon Ice Cap (Fig. 1), a dome-shaped ice
cap that reaches maximum altitude of 1921 m and is the highest point on the island (Dyke, 1999; Boon et al., 2010;
90 Dowdeswell et al., 2004). The ice cap is 350 – 880 m thick and is drained by numerous outlet glaciers along the east coast
that are constrained by the subglacial Cunningham Mountains (Dyke, 1999; Dowdeswell et al., 2004).

92 The polar desert climate of Devon Island is uniquely suited to study cold and polythermal based ice cap glaciation and
associated landform assemblages (Dyke, 1999; Boon et al., 2010). Minimal precipitation and vegetation on Devon Island
94 have prevented the significant degradation of this landscape since ice exposure approximately ~8000 radiocarbon years
before present (BP) (Fig. 1) (Dyke, 1999), allowing for landforms to be studied from the km- to cm-scale (Osinski et al.,
96 2005). However, the geological record on Devon Island, specifically the record of past glacial activity, is sparse; striations,
bedrock scours, and moraines are the only documented landforms on the island suggestive of glacial flow and they are rare,
98 constrained to the coastal areas (Dyke, 1999). Exceptionally well-preserved networks of subglacial and lateral meltwater
channels have also been documented in the inland plateau region of the island (Dyke, 1999; Grau Galofre et al., 2018). On
100 the regional scale, erratics scattered throughout the islands that make up the Canadian Arctic Archipelago, the Queen
Elizabeth Islands (QEI), have provided some evidence towards glaciation during the Last Glacial Maximum (LGM);
102 however, the conspicuous lack of glacial landforms on the islands has caused some to question the existence of an ice sheet
over the QEI in the past (Dyke, 1999).

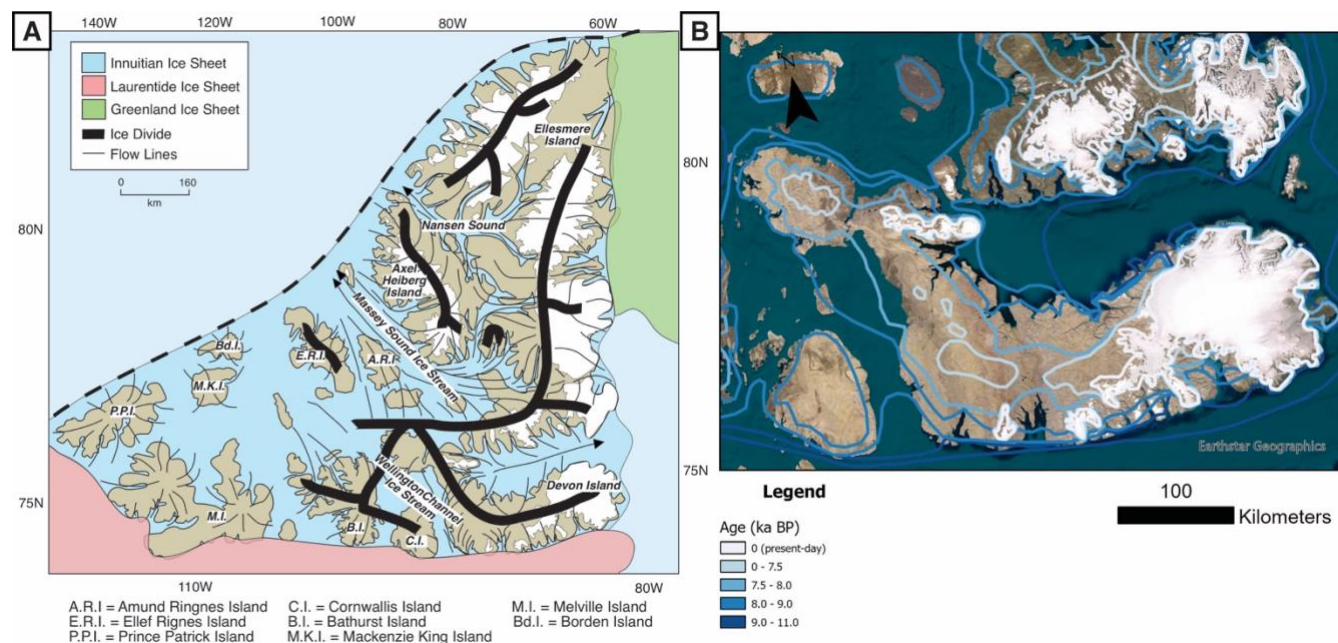
104 **1.2.2 Glacial history**

To date, only a handful of studies have investigated the extent and dynamics of glaciation in the QEI. Blake (1970) proposed
106 the presence of the Innuitian Ice Sheet (IIS), an extensive ice sheet that covered the entirety of the QEI during the LGM that
coalesced with the Laurentide Ice Sheet to the south and the Greenland Ice Sheet to the east (Fig. 1). Alternatively, England
108 (1976) suggested that glaciation in the QEI was significantly less extensive than the IIS of Blake (1970), stating that



geological evidence of widespread glaciation is conspicuously absent except near fjords (England et al., 1991; England,
110 1976). Instead, the author proposed the existence of the Franklin Ice Complex, a series of discrete island-bound ice caps that
may have converged but never fully coalesced during the LGM (England, 1976). The debate over the extent of glaciation in
112 the QEI culminated in general acceptance of the IIS, where the relatively large size of some major inlets (up to 70 km long
and 10 km wide) and radiocarbon ages of marine shells that become younger in the direction of ice retreat (eastward) were
114 cited as evidence for a single, contiguous ice sheet rather than multiple discrete ice caps (Blake, 1970; England, 1998). Later
work in the QEI focussed on determining the configuration and extent of the ice sheet, and its relationship with the
116 Laurentide and Greenland ice sheets (Dyke et al., 2002, Dalton et al., 2022).

It is now generally accepted that the IIS was comprised of two sectors: a northern alpine sector, where ice flowed outward
118 from the mountains on Axel Heiberg and Ellesmere Islands, and a southern lowland sector that completely covered the
western QEI and filled in the inter-island channels (Dyke et al., 2002; Simon et al., 2015, Dalton et al., 2022). The alpine and
120 lowland sectors of the IIS have been proposed to have reached peak thicknesses of ~1600 m and ~1330 m, respectively, in
contrast to the Laurentide Ice Sheet peak thickness of over 4500 m (Simon, 2004; Simon et al., 2015). The contrast in
122 thickness between the two contemporaneous ice sheets has been attributed to efficient drainage via ice streams in the inter-
island channels that likely reduced thickening of the IIS (Dyke et al., 2002). For example, the Wellington Channel
124 immediately west of Devon Island (Fig. 1) was occupied by a 600 m thick ice stream (England et al., 2006) that impacted the
drainage and flow of grounded ice on surrounding islands. This effect may provide at least a partial explanation as to the
126 paucity of glacial landforms on Devon Island.



128 **Figure 1. A) Map of the QEI glaciated by the IIS during the LGM, ~25Kyr BP. The IIS coalesced with the Laurentide Ice Sheet directly to the south of Devon Island, and to the northeast with the Greenland Ice Sheet. Note locations of ice divides along the**



130 **centre of each island, and the locations of ice streams in the major inter-island channels. Adapted from** England et al., (2006). **B)**
132 **Satellite image of Devon Island with isochrons illustrating radiocarbon dates of glacial retreat at the end of the LGM. Modified**
from (Dyke, 1999)

Collapse of the IIS began around 11 ka BP in the western section of the ice sheet and culminated to roughly its present-day
134 configuration by around ~7.5 ka BP (Fig. 1) (England et al., 2006). While the general timeline and extent of the IIS has been
broadly investigated, the pattern of glacial advance and retreat on individual islands, in particular Devon Island, has yet to be
136 fully explored.

1.2.3 Devon Island subglacial channels and previous work

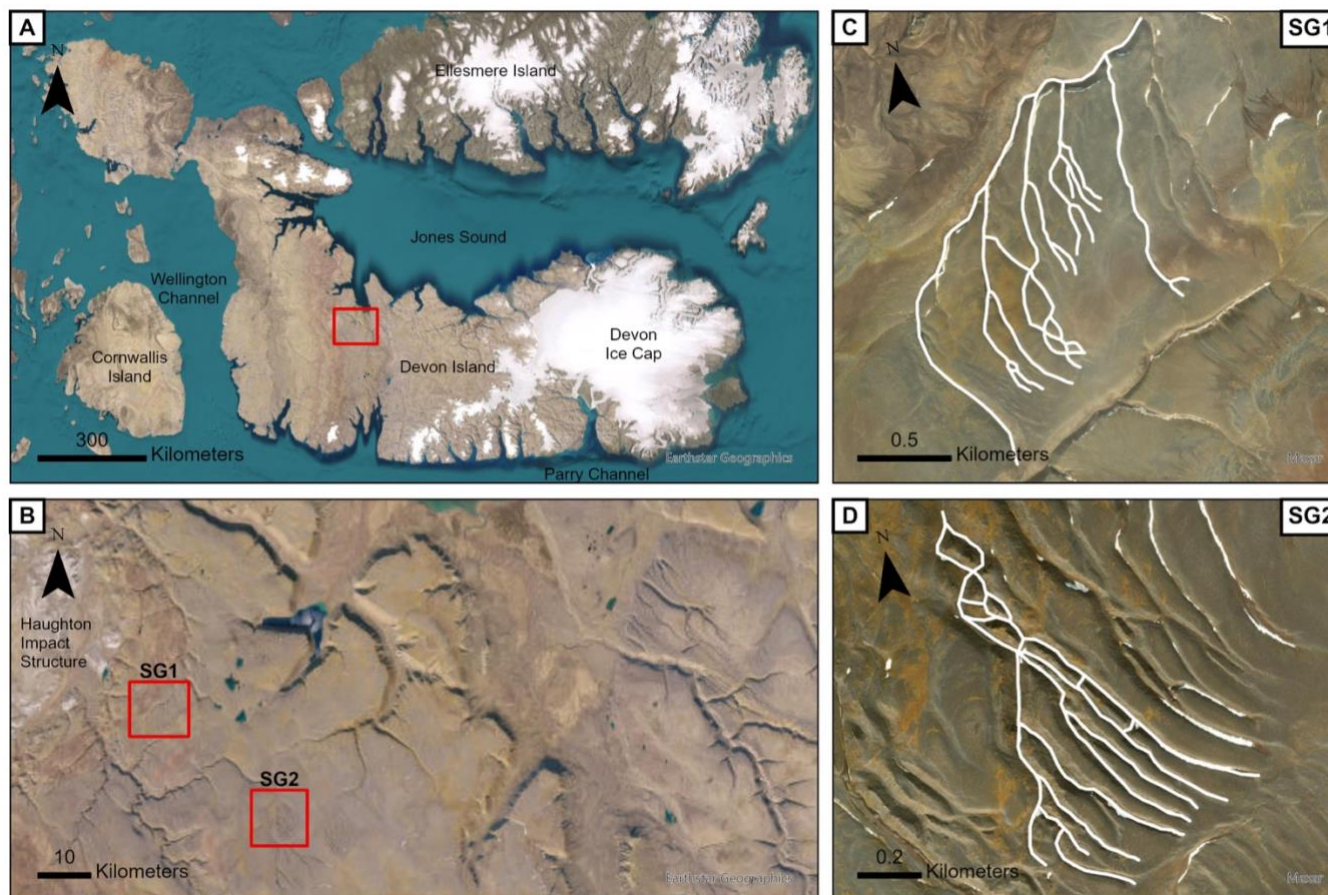
138 Very little work has been done on Devon Island to map and characterize glacial landforms and their distribution in the
landscape. Dyke (1999) produced the only published glacial geological map of Devon Island in an attempt to resolve the
140 debate surrounding the existence of the IIS. He proposed a basal thermal zonation of the ice sheet, comprised of an outer,
warm-based zone and an inner, cold-based zone. The warm-based zone is identified by weak to moderate glacial scouring
142 that formed rock basin lakes and striations, as well as the presence of end moraines. Major fjords incising the north and south
coasts of Devon Island also provide evidence of glacial scouring in the outer zone (Fig. 2). The inner, cold-based zone
144 occupied Devon Island's highland plateaus, and is characterized by the presence of lateral meltwater channels and smooth,
wide interfluves (Fig. 2). While Dyke's work offered significant evidence in favour of the IIS through dating shells and
146 identification of various glacial flow features along the coast, the resolution of the mapping is too low for an in-depth
investigation into glacier and meltwater dynamics that occurred on Devon Island during the LGM.

148 Other researchers studied meltwater channels on Devon Island motivated by their similar morphology to valley networks on
Mars (Lee et al., 1999; Lee & Rice, 1999); however, these studies focussed only on large-scale morphological comparisons
150 and exist only as conference abstracts. More recently, Grau Galofre et al. (2018) conducted the first in-depth investigation of
subglacial channels on Devon Island and their role in subglacial drainage. The authors provided field descriptions of
152 channels and proposed a set of criteria to identify subglacial channels using remote sensing techniques. These criteria include
the magnitude of undulation, described as the degree to which the longitudinal profile of a channel undulates, deviation of
154 flow lines from topography, and width to depth ratio that describes the shape of a channel cross-section from V- to U-
shaped, defined as the shape factor (Grau Galofre et al., 2018). Their work established a framework that enhances the ability
156 to identify subglacial channels in the field and/or through remote sensing, and it is that framework on which this study aims
to expand.

158 This study focusses on two unnamed networks of subglacial channels on central Devon Island (Fig. 2), designated as
Subglacial Channel Network 1 (SG1) and Subglacial Channel Network 2 (SG2) (Fig. 2). These networks are highly
160 directional, isolated features that are comprised of anastomosing, short, straight, and regularly spaced tributary channels that
drain into a deeper and wider main stem channel. SG1 and SG2, along with other networks in the region, provide an



162 opportunity to expand the current set of criteria used to identify subglacial channels, enhance our understanding of meltwater
dynamics under cold- to polythermal-based ice sheets, and further constrain the glacial history of Devon Island.



164
166 **Figure 2.** A) Satellite image of Devon Island. Note the Devon Ice Cap on the eastern end of the island. B) General overview of study
168 area; note the Haughton Impact Structure on the left-hand side of the image and the well-developed fjords along the centre and
top of image, and several lakes near fjords. Locations of SG1 and SG2 in red boxes. C) SG1; note highly directional tributary
channels connected to the main stem. Paleoflow towards the top of the image. D) SG2; note the labyrinth terrain towards the top
of the image. Images are 30 cm resolution MAXAR imagery.

170 2 Methods

A two-week field work campaign was conducted in July 2022. Prior to fieldwork, the site was characterized using remote
172 sensing imagery and topographic data from Maxar (30 cm resolution), sourced from Google Earth, and stereo-derived
topography data from the ArcticDEM (2 m/pixel). From remote sensing data, we defined regions of interest around SG1 and
174 SG2 to be visited in the field. Due to accessibility constraints, only SG1 was visited in person. LiDAR data of SG1 and SG2
was collected in the field using a Matrice 300 RTK DJI Pilot drone equipped with a DJI Zenmuse L1 LiDAR at an altitude
176 of 100 m. The Zenmuse L1 camera has down to 3 cm resolution with a horizontal accuracy of 10 cm and vertical accuracy of



5 cm. We defined an acquisition campaign with the specific objective of capturing the entirety of each of the subglacial
178 channel networks identified via remote sensing before fieldwork began (SG1 and SG2). The drone flight path for each
network began at the headwaters and flew along transects perpendicular to the channel network, working towards the main
180 stem, with the camera pointing in the nadir direction. We collected a total of 1017 images for SG1 and 499 for SG2. GPS
data for the LiDAR images was collected continuously during flight using 83 waypoints for SG1 and 58 waypoints for SG2.
182 Drone image data was processed using DJI Terra to create high-resolution (cm-scale) DEMs. Raw drone LiDAR data was
processed using DJI Terra into point cloud files (.LAS). Workflow for point cloud to raster processing is as follows: Point
184 cloud files were loaded into ArcMap 10.8 and a LAS dataset was created using the “Make LAS Dataset Layer” tool in the
Geoprocessing toolbox, filtered for Last Returns only. A raster (.TIF) was developed from the filtered LAS dataset using the
186 “LAS Dataset to Raster” tool (value field: Elevation, cell arrangement type: IDW, data output as floating point, cell size:
0.25 m). Hillshade DEMs were produced from the raster using the “Hillshade” function in ArcMap and overlain by the
188 original in a graded colour scheme to assist in visualization. The final resolution of the DEMs were 0.41 m/pixel (SG1) and
0.28 m/pixel (SG2). The projection used for analyses was WGS 1984 UTM Zone 16. ArcticDEM (2 m resolution) and
190 Google Earth (MAXAR imagery, 30 cm resolution) were used as the main datasets for regional context.

Channels were delineated manually by creating polylines and tracing the centre lines of each channel on the DEM data
192 acquired from last sections. Cross-section profiles were drawn on the raster created from the LiDAR data using the
“Interpolate Line” function from the 3D Analyst tool. Cross-section profiles were drawn approximately every 50 – 100 m
194 along each channel segment and width and depth measurements were extracted manually from each cross-section using the
“Profile Graph” function from the 3D Analyst tool, following the convention of (Williams and Phillips, 2001). Minimum
196 width was measured from the lowest valley rim straight across to the adjacent wall, and depth was measured as the
difference between the lowest elevation (channel floor, ignoring inner channels if present) and the average elevation of the
198 highest and lowest valley rims. Cross-sectional area was calculated in Microsoft Excel as the product of depth and height.
Longitudinal profiles were carefully drawn along the centreline of each channel using the same “Profile Graph” function
200 introduced above. The number of anastomoses of tributary channels were counted and divided by the maximum length
(furthest distance from tributary headwaters to the main channel) of the network to calculate the ratio of the degree of
202 anastomosis of the channel to the total channel length, a novel metric hereafter referred to as the anastomosing ratio.

3 Results

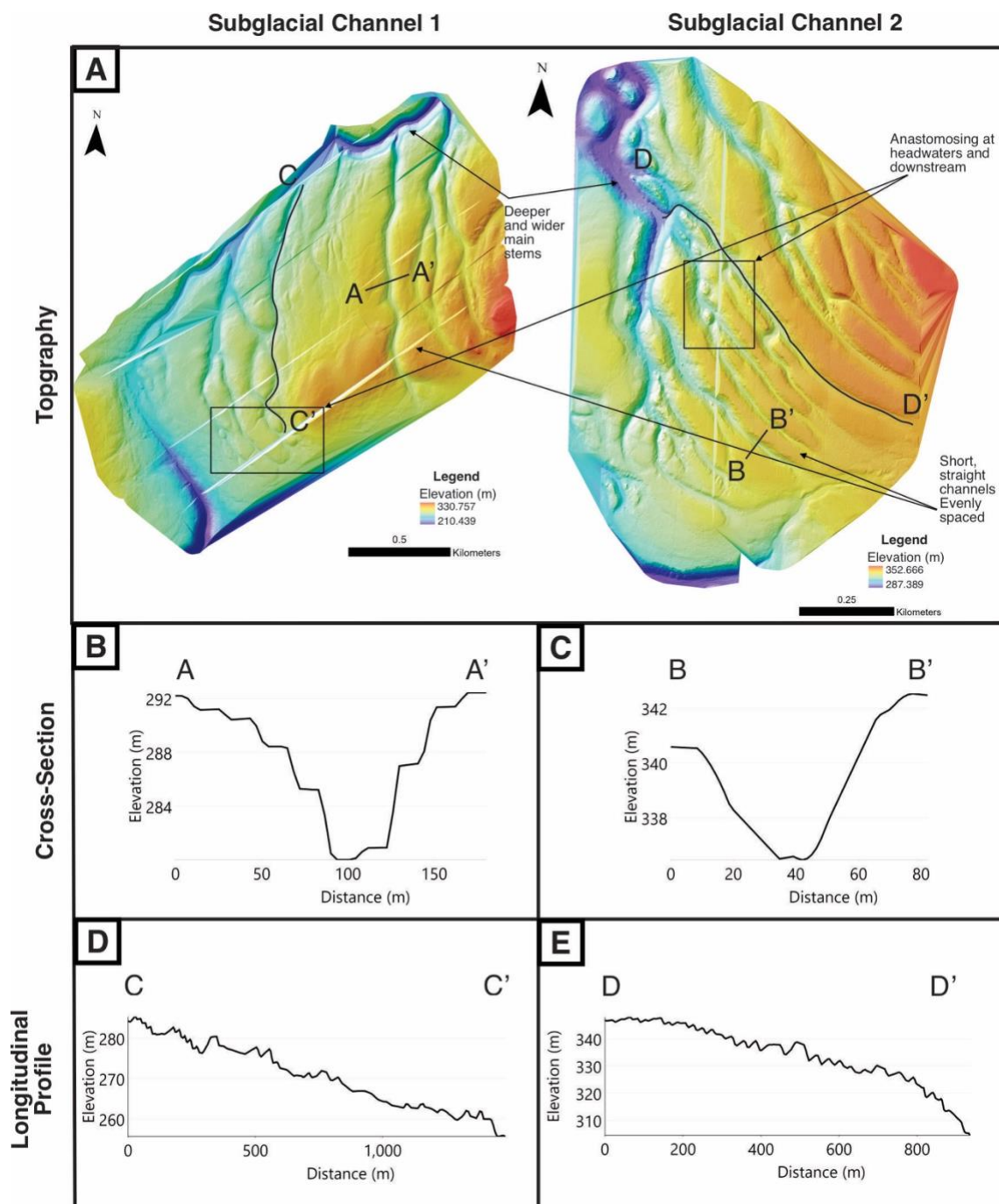
204 3.1 Description of morphology from field and remote sensing data

3.1.1 Planform morphology and network topology

206 The main stems of SG1 and SG2 are generally deeper and wider than the tributary channels, which are relatively short,
straight, and evenly spaced (Fig. 3). This is readily observed in the DEMs where the floors of the main stems are



208 significantly lower in elevation than the tributaries (Fig. 3). Most channels exhibit an anastomosing pattern, consisting of
multiple connected channel sections that we observe to occur primarily at the headwaters of the network (Fig. 3).
210 Anastomoses are defined here as locations where a single-thread channel divides and re-merges downstream, distinct from
fluvial systems where anastomosing occurs as a result of increased bedload and channel aggradation, or avulsions associated
212 with highly sinuous meandering rivers (Makaske, 2001). Channel junction geometry at anastomosing sections is
characterized by relatively flat channel floors and slightly wider channel widths (i.e., no over-deepening or significant
214 widening is observed where channels merge). Anastomoses are less common in SG1 than in SG2 but can be observed in
both networks near the tributary headwaters and downstream towards the main stem (Fig. 3).
216 In satellite imagery SG1 and SG2 are observed as isolated channel networks and are not located within any significant
drainage basin, although connections between some valleys can be observed (Fig. 2). Regionally, SG1 and SG2 incise into
218 the flat-lying stratigraphy of carbonate rocks of the Arctic Platform with no observable curvature that could serve as a
drainage basin. Moreover, paleoflow of both networks is oriented towards the northwest, perpendicular to the drainage
220 divide that runs roughly west-east along the centre of the island (Fig. 1), and towards small lakes and major fjords that drain
into Thomas Lee Inlet (Fig. 2). At the local scale, channels lie oblique to the local topographic gradient and, in the case of
222 SG1, cut through a topographic ridge near the headwaters of the easternmost channels (Fig. 3). No evidence of glacial
scouring or depositional features such as eskers was observed at the study areas; the only other related landforms near SG1
224 and SG2 are lateral meltwater channels, which were observed via remote sensing and traversed in the field. These channels
are significantly shorter than those in the subglacial channel networks and are typically part of a series of lateral meltwater
226 channels that drain into one of the many valley networks cut into the Devon Island Plateau.



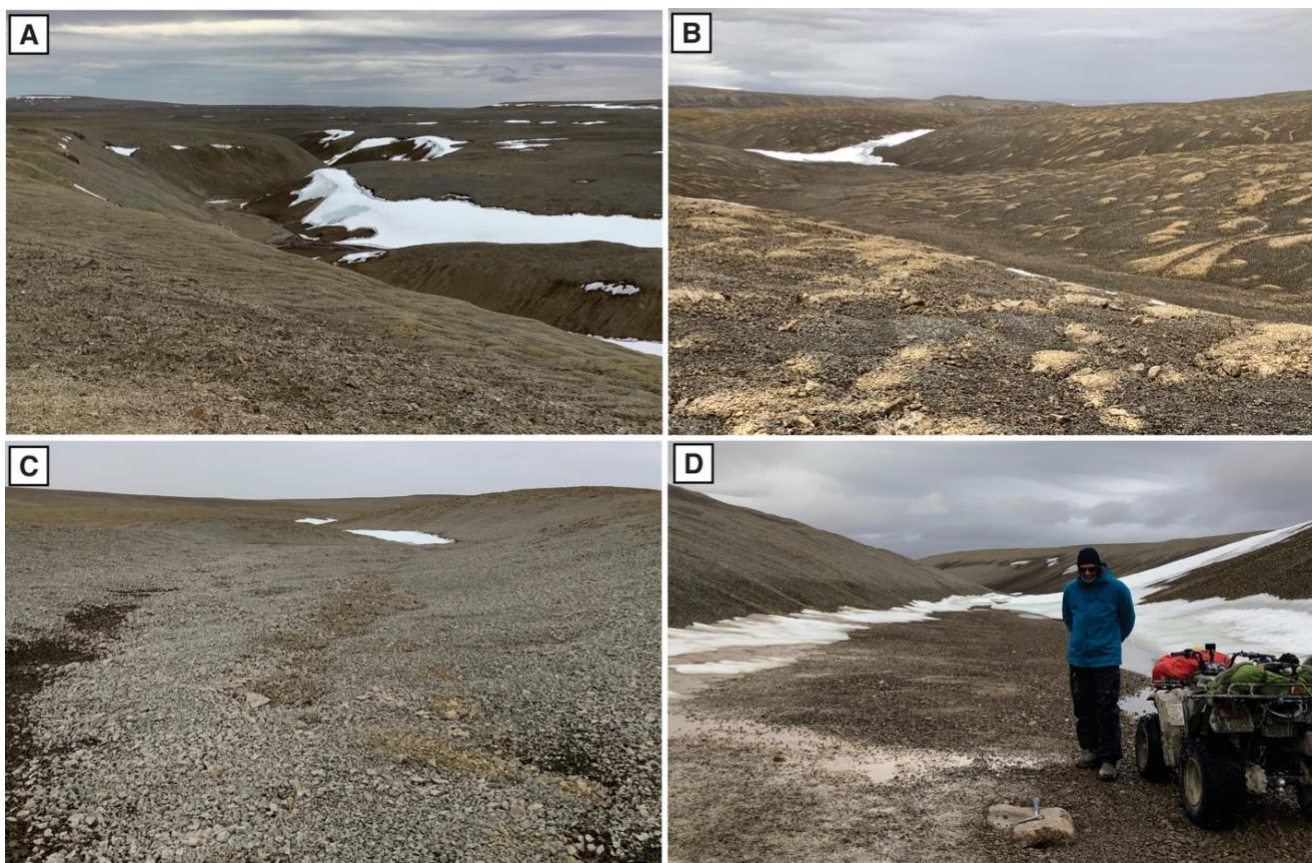
228 Figure 3. A) Morphological characteristics of SG1 (left) and SG2 (right). Main stem channels are deeper and wider than
 230 tributaries, which are short, straight, and evenly spaced. Channels exhibit anastomosing patterns at both headwaters and
 232 downstream reaches. Channels are delineated by black lines. B) and C) Example cross-section profiles A-A' and B-B' of channels
 in each network. X-axis represents channel width in metres, y-axis represents elevation in metres. D) and E) Example longitudinal
 profiles C-C' and D-D' of channels in each network. Note the convex shape and presence of undulations. X-axis represents
 distance along stream in metres, y-axis represents elevation in metres.



234 3.1.2 Cross-sectional profiles

236 Cross-sectional profile geometry is variable but is typically trapezoidal (flat-bottomed) in shape (Fig. 3). Rare sharp-
bottomed (V-shaped) cross-sections were observed. Some inner channels were observed in cross-sections obtained from the
238 DEMs; the channels are less than a metre in width and depth and were rarely observed in the field. In the field, inner
channels were only observed within the main stem (Fig. 4A) or close to the main stem in the more developed tributaries; no
inner channels were observed near the tributary headwaters (Fig. 4B-C). Water within the inner channels was likely sourced
240 from snow melt; snow patches were uncommon but, where present, filled some depressions along the contact between
channel wall and floor to depths of tens of centimetres (Fig. 4D).

242 Longitudinal profiles of tributary channels are typically convex, although some in SG1 are slightly concave (Fig. 3D-E).
Profiles are irregular but not stepped, and do not contain any knickpoints; however, undulations are common in both
244 networks, with a statistic mode of 1–2 m and a maximum of 4 m in height. In SG1, maximum (3 – 4 m) undulations occur at
locations where anastomoses are present (i.e., where two channel segments converge/diverge) and are associated with
246 slightly deeper and wider cross-sectional profiles (Fig. 3B-C). Anastomosis is less prevalent in SG2 and is not readily
observed in the longitudinal profiles, which are more uniform than SG1.



248



250 **Figure 4. Example field photos of SG1. A) Main stem of SG1 facing approximately northeast. B) Example of the flat-bottomed**
252 **tributary channels and unincised interfluves that comprise the subglacial channel networks on Devon Island. C) Shallow**
254 **headwaters of a tributary channel; note how channel width remains relatively constant while depth changes significantly in**
256 **comparison to B). D) Flat-bottomed channel floor with snow accumulation along the sides of the channel; note person and ATV for**
258 **scale.**

254 3.2 Channel morphometry

The main stem of SG1 is ~2.3 km long. It has a depth range of 7.2 – 36 m, with an average of 20 m. The average main stem
256 width is 96 m with a range of 44 – 172 m. The cross-section area of the main stem varies between 475 m² and 6146 m²,
averaging 2255 m². There are four tributary channels within SG1. Tributary channels of SG1 have an average length of 1.3
258 km and range in length from 0.97 – 1.6 km. Channel depth varies between 0.47 m to 16 m, averaging 9.6 m, and width has a
range of 7.7 – 120 m with an average channel width of 68 m. There are two outliers with depths of 140 m and 205 m.
260 Channels have an average cross-sectional area of 1153 m² and a range of 3.64 m² to 11288 m². The anastomosing ratio for
SG1 is 4.5.

262 The main stem of SG2 is 0.95 km in length. The depth ranges between 4.2 m and 27 m, averaging 17 m. The average width
of the main stem is 76 m, with a range of 24 m to 148 m. The cross-section area of the main stem is on average 1470 m² and
264 varies between 100 m² to 3778 m². There are seven tributary channels within SG2. SG2 tributary channels range in length
between 0.43 – 0.89 km, with an average of 0.62 km. Depth varies between 1.1 m and 18 m, with an average depth of 8.5 m.
266 Channel width range is 12 m – 82 m with an average of 36 m. Cross-sectional area is on average 345 m², with a range of 15
m² – 1458 m². The anastomosing ratio for SG2 is 10.2.

268 3.3 Scaling relationships

In an effort to establish quantitative comparisons between fluvial and subglacial drainage systems, we analysed width and
270 depth data by adapting scaling relationships traditionally applied to fluvial systems; specifically, we assessed power-law
relationships between width, distance, and drainage area for each network (Wright et al., 2022). The fluvial scaling
272 relationships follow the power-law equations for Channel Geometry (1) and Basin Hydrology (2):

$$W = k_w Q^b, \quad (1)$$

$$274 Q = k_q A^c, \quad (2)$$

where Q = discharge, A = drainage area, W = width, k_q and k_w are dimensional constants, and c and b are dimensionless
276 constants (Whipple and Tucker, 1999). In the fluvial literature, the basin hydrology scaling (Eq. 2) represents the
relationship between the size of the drainage area and bank-full discharge in the river, establishing a mass-balance scaling
278 (Dodov and Fofoula-Georgiou, 2004). The channel geometry scaling equation (Eq. 1) (also termed hydraulic geometry) of
a river describes the relationship between bank-full discharge and channel width (Leopold and Maddock, 1953), and arises
280 from river hydraulics.

Since SG1 and SG2 currently do not contain any flowing water to apply these scaling relationships directly, and we are
282 assessing the scaling relationships through the lens of a subglacial system that no longer exists, we have employed proxies to

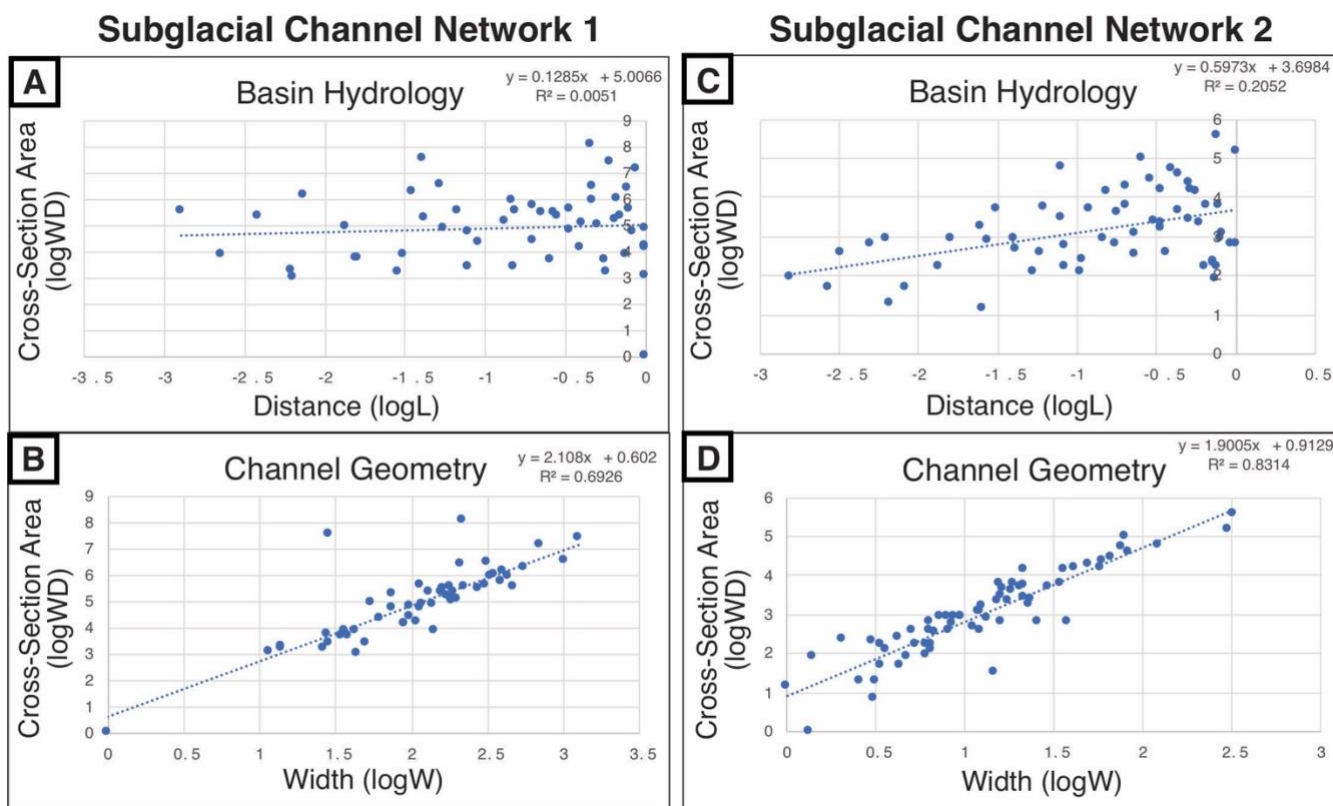


284 describe these relationships: as a proxy for bank-full discharge, cross-sectional area of the channels is used, and distance
286 downstream was used as a proxy to describe the size of the drainage area (drainage area and length of a river system are
linked through Hack's law). Note that drainage area as a topographic construct limiting the source regions for the subglacial
channel networks studied was not observed to exist.

The basin hydrology scaling for SG1 exhibits no correlation between paleo discharge and drainage area (Fig. 5A), with an R^2
of 0.005. The calculated power law exponent for these data is 0.13. Channel geometry scaling reveals a linear relationship
between channel width and discharge ($R^2 = 0.69$) (Fig. 5B) and the power-law exponent is 0.64.

SG2 basin hydrology scaling also reveals a weak correlation between discharge and size of the drainage area (Fig. 5C), with
an R^2 of 0.21. The power law exponent for this scaling is 0.60. Similar to SG1, the channel geometry scaling exhibits a linear
relationship between discharge and channel width for SG2 (Fig. 5D). The R^2 value for this scaling is 0.83 and the power law
exponent is 0.69.

294



296 **Figure 5. Scaling relationships of SG1 and SG2. A) and C) Basin hydrology scalings for SG1 and SG2. Cross-sectional area of the**
298 **channel (y-axis) is used as a proxy for bank-full discharge, represented as the logarithm of width (m) multiplied by depth (m).**
Distance downstream (x-axis) is used as a proxy for drainage area and is represented as the logarithm of distance (m) from the
300 **headwaters. B) and D) Channel geometry scalings. Cross-sectional area (y-axis) is a proxy for discharge and calculated the same as**
panels A and C. Width (x-axis) is measured in metres from the lowest valley wall straight across the channel and plotted as the
logarithm.



302 4 Discussion

We have provided the most in-depth analysis of subglacial channels on Devon Island, building on the work of Grau Galofre
304 et al., (2018). For the first time, we have tested fluvial scaling relationships in subglacial channels in an effort to further
enhance the distinctive criteria between fluvial and subglacial channels. In the following sections, we discuss the
306 distinguishing characteristics of subglacial channels in terms of morphology, morphometry, and scaling relationships, and
the implications for meltwater drainage dynamics on Devon Island under the cold- to polythermal-based IIS.

308 4.1 Morphology

The flat-bottomed cross-sections, undulating long profiles, and short, straight anastomosing character of the tributary
310 channels of SG1 and SG2 are consistent with formation by pressurized subglacial flow (Sugden et al., 1991; Grau Galofre et
al., 2018; Greenwood et al., 2007; Lewis et al., 2006). The presence of multiple anastomoses along the lengths of the
312 tributary channels, especially towards the headwaters, is distinct from fluvial systems where anastomosing typically occurs
in the distal reaches of long-lived, stable rivers (Makaske, 2001). In the case of flooding rivers, intense overbank flow incises
314 new channels (anabranches) that eventually widen and deepen downstream as they become more sinuous (Schumm et al.,
1996). Anastomosing of the short and straight channels in SG1 and SG2 indicates that the flow was high energy and
316 relatively stable as the channels do not evolve downstream. Moreover, anastomosis of subglacial conduits has been linked to
discrete recharge events by over-pressurized moulins (Gulley et al., 2012). Drainage of tributary channels into a larger main
318 stem is also a common feature of channelized subglacial drainage (Shreve, 1972) that is readily observed in all Devon Island
channel networks.

The isolated nature of subglacial channel networks on Devon Island as well as the lack of glacial landforms in the vicinity of
320 SG1 and SG2 other than lateral meltwater channels, based on both field observations (Fig. 4) and high-resolution remote
sensing data (Fig. 2), is consistent with the two-fold thermal zonation of the IIS proposed by Dyke (1999). Although thin,
322 polar ice sheets tend to be colder along the margins (e.g., Atkins, 2013), this distinctive two-fold zonation is readily observed
when comparing the environment surrounding SG1 and SG2 to the coastal areas of Devon Island; the highland plateaus are
324 dominated by meltwater channels and broad, unincised interfluves (Figs. 2B-D) while lakes, moraines, and striations
populate the coastline and plateaus directly near major inlets, remnants of former outlet glaciers (Fig. 2B) (Dyke, 1999).
326 Moreover, ice streams such as the Wellington Channel Ice Stream that occupied the channels surrounding Devon Island (Fig.
2A) likely increased the efficacy of meltwater drainage inland by concentrating fast flowing ice along the coastline and
328 offshore, influencing ice-sheet dynamics and playing a role in maintaining a cold-based core and warm-based margin
(Kleman et al., 1999; Kaplan et al., 2001; Hughes, 1998). For example, Thomas Lee Inlet, ~20 km north of SG1 and SG2
330 (Fig. 2A), is among many inlets along Devon Island's coastline fed by wide, flat-bottomed fjords, with source region
332 characterized by small lakes, offering observational evidence of a contrasting thermal regime to that of the inland area. The

channels in SG1 and SG2, therefore, formed under the cold/polythermal-based zone of the IIS that temporarily
334 accommodated channelized meltwater flow, while glacial sliding occurred at the nearby Thomas Lee Inlet.

The morphologies discussed here are comparable to subglacial meltwater channels carved into bedrock by temporary
336 subglacial meltwater accommodation (i.e., episodic release) in other polar regions (e.g., Kirkham et al., 2020; Sugden et al.,
1991; Gulley et al., 2012). Our data is consistent with previous work that identified the flat-bottomed profiles and undulating
338 longitudinal profiles of another subglacial channel network on Devon Island (Grau Galofre et al., 2018). Although the
previous study presents lower-resolution LiDAR data than what we have presented here, we can unequivocally establish that
340 SG1 and SG2 are networks of subglacial channels and therefore provide a basis to test the two fluvial scaling relationships.

4.2 Channel geometry

342 The scaling relationships of SG1 and SG2 are consistent with each other and are distinct from those reported in the fluvial
literature for river systems (Whipple and Tucker, 1999). The pioneering work of Leopold & Maddock (1953) on hydraulic
344 geometry, followed by numerous studies thereafter (see Gleason, 2015 for a review), relates river discharge to width, depth,
and water velocity as a power-law (Eq. 1 and 2). The hydraulic geometry of a river presents a strong correlation between
346 discharge and the size of the channel, where increases in discharge will directly influence river width, depth, and/or velocity
(Wright et al., 2022). Our Channel Geometry analysis of SG1 and SG2 displays a strong correlation between channel cross-
348 sectional area, utilized as a proxy for subglacial discharge assuming the channels flowed at bank-full width, and channel
width (Figs. 5B, D), with an exponent of the power-law Eq. (1) ($b = 0.64$ and 0.69) for both systems that is greater than, but
350 comparable with, the fluvial range ($b = 0.4 - 0.6$), indicating a stronger coupling of discharge and width than what is
observed in a fluvial system. This could explain the consistency of main stem channel width in SG1 and SG2 with distance
352 along the channel axis, even when discharge increased downstream with input from tributary channels. Wright et al. (2022)
propose that in rivers bound by bedrock increased discharge is accommodated by vertical (downward) erosion while width
354 remains relatively constant. For subglacial channels, downward incision into bedrock as well as upward erosion into the
overlying ice compensate for increased discharge in the channel and maintain channel widths downstream (Rothlisberger,
356 1972). This has been observed in the Labyrinth in the Dry Valleys of Antarctica, where increasing cross-sectional area of
channels is the result of deepening rather than widening (Kirkham et al., 2019).

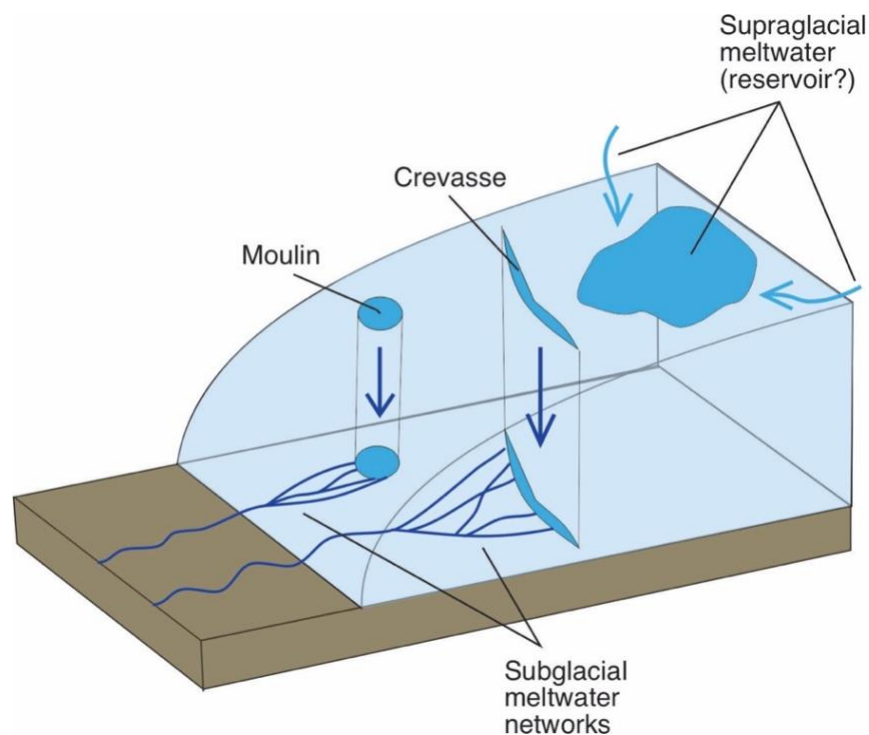
358 4.3 Basin hydrology and channel formation

This novel application of the basin hydrology scaling relationship reveals a markedly different relationship for the Devon
360 Island channels than what has been observed in the fluvial literature. In a fluvial system, increasing the size of the drainage
area progressively increases the bank-full discharge of a river downstream, as more water is sourced from within the
362 drainage area (e.g., Dodov & Foufoula-Georgiou, 2004; Lee et al., 2009; Solyom, 2004). We do not see any indication of
this relationship in the SG1 and SG2 data. Instead, there is a distinct weak correlation between the size of the drainage area
364 and the bank-full discharge in the channel (Figs. 5A, C) and the calculated power law exponents in Eq. (2) ($c = 0.13$ and



0.60) are significantly less than the fluvial range ($c = 0.7 - 1$). Dodov & Fofoula-Georgiou (2004) describe a strong linear
366 relationship between contributing area in the Neosho and Osage River basins in Kansas and Missouri, USA, and bank-full
discharge of rivers draining these basins, which they attribute to the downstream increase of channel asymmetry and
368 increasing instability of the river itself. If SG1 and SG2 were indeed formed by intense but short-lived episodic outbursts,
then the stability of the flow would not play as much of a role in modifying channel geometry as it would in a system with a
370 long-lived sustained flow, such as a meandering subaerial river (Dodov and Fofoula-Georgiou, 2004). Moreover, the
contrast of the Devon Island subglacial system to a fluvial system implies that there are other controls active in a subglacial
372 system in terms of basin hydrology and water source.

Further application of the basin hydrology scaling relationship to other subglacial systems would be useful to compare to the
374 formation and evolution of the Devon Island channels and further develop criteria to distinguish subglacial channels from
remote sensing data. In the absence of this data, we discuss the formation of SG1 and SG2 based on our data and
376 observations presented here, known conditions of the IIS, and geology of the study location. Many studies of cold-based ice
sheets attribute the formation of channelized drainage systems with similar morphologies to SG1 and SG2 to the episodic
378 drainage of subglacial lakes (e.g., Hogan et al., 2022; Kirkham et al., 2019; Larter et al., 2019; Lewis et al., 2006; Sugden et
al., 1991)); however, while we cannot rule out the presence of a major subglacial lake, modern lakes on Devon island are
380 relatively small and concentrated along the coast, and there is no topographical evidence of a past major inland basin on
Devon Island that could have fed the subglacial channel networks (Figs. 2A-B). Instead, we suggest that the meltwater is
382 supraglacial in origin and routed through a point or line source, such as a moulin or crevasse (Fig. 6). The weak correlation
between drainage area and discharge in the Basin Hydrology scaling relationship hence suggest that basal melt did not play a
384 role in sourcing these channels, which is once more coherent with a mostly cold based IIS, with occasional basal meltwater
presence due to surface melt. (Fig. 5).



386

388 **Figure 6. Cartoon illustrating routing of supraglacial meltwater in a cold-based ice sheet via moulins and crevasses. Modified from Livingstone & Clark (2016).**

Although this scaling relationship and power-law equation has not yet been applied to other subglacial systems, supraglacial drainage into a subglacial system similar to what we propose here has also been documented in the Greenland Ice Sheet (e.g., Bartholomew et al., 2012; Das et al., 2008; Zwally et al., 2002), Antarctica (e.g., Langley et al., 2016; Stokes et al., 2019; Tuckett et al., 2019), and the Canadian High Arctic (e.g., Bingham et al., 2008; Wyatt & Sharp, 2015). While it is well documented in Greenland, the effect of supraglacial meltwater drainage on ice velocity variability in other more remote polar environments is not as readily observable. In the Canadian Arctic, at the John Evans Glacier on Ellesmere Island, seasonal basal motion was locally enhanced by supraglacial drainage (Bingham et al., 2008), and at the Devon Ice Cap extensive crevassing and thinner ice near the margin of the ice cap allow for penetration of surface meltwater to the bed, contributing to an increase in ice velocity variability (Wyatt and Sharp, 2015). In Antarctica, supraglacial lakes have been observed to freeze and melt over seasonal cycles or drain over a matter of days through englacial pathways (Langley et al., 2016).

Episodic drainage of surface meltwater to the ice-bed interface accelerates ice flow velocity (and therefore glacial erosion) by increasing water pressure at the bed which induces sliding (Cowton et al., 2012). However, there is no evidence of glacial sliding near SG1 and SG2 indicating that frozen-bed conditions prevailed in the channel interfluves (Figs. 2C-D, 3A, 4B). This effectively contained the meltwater within an efficient, channelized subglacial drainage system associated with low water pressures and reduced basal sliding (cf., Schoof, 2010; Jansen et al., 2014). Therefore, a highly efficient subglacial drainage system able to temporarily accommodate an influx of meltwater without increasing ice flow velocity (or

404



immediately returning to no-flow conditions) would be required to account for the lack of glacial flow landforms near the
406 subglacial channel networks on Devon Island. An example of such a mechanism of brief but rapid glacial acceleration was
observed at five outlet glaciers in the Antarctic Peninsula and was directly linked to drainage of supraglacial lakes (Tuckett
408 et al., 2019). The rapidity of this event (< 6 days) and immediate return to pre-event ice velocities suggests that glaciers can
temporarily operate under a highly efficient subglacial drainage system to accommodate large volumes of supraglacial
410 meltwater (Tuckett et al., 2019). However, the timing of meltwater reaching the bed is also an important control on drainage
and ice velocity dynamics. Supraglacial meltwater routed to the bed late in the melt season when the subglacial drainage
412 system is established (i.e., efficient) will have less of an effect on the magnitude of velocity change than early in the melt
season, when the subglacial drainage system is not fully developed (i.e., inefficient) (Wyatt and Sharp, 2015; Lewington et
414 al., 2020). Thus, we suggest that SG1 and SG2 had to have formed by a large-scale meltwater release event in the late stages
of the melt season that briefly accommodated supraglacial meltwater input without inducing basal sliding.

416 When taken together, we propose that our observations of SG1 and SG2 – in particular their isolated nature and short,
straight, and anastomosing morphology of the channels – is most consistent with periods of intense erosion associated with
418 episodic but locally intense drainage of supraglacial meltwater through moulins or crevasses (Fig. 6). Our data is consistent
with previous work, and we propose a formative process to describe the development of subglacial channel networks on
420 Devon Island. Modelling by (Beaud et al., 2018) demonstrates that high-frequency, small-scale meltwater input (e.g., diurnal
or seasonal flooding), rather than low-frequency, large-scale input (e.g., catastrophic flooding), is sufficient to carve bedrock
422 channels up to hundreds of metres wide and tens of metres deep via surface melt. The morphometry of channels in SG1 and
SG2 is well within the range for inception and development by seasonal meltwater erosion, and the lack of evidence of a
424 large subglacial meltwater reservoir aligns with the cold and dry climate of the Canadian High Arctic and dominantly cold-
based thermal regime of the Innuitian Ice Sheet. Therefore, it is more likely that supraglacial or englacial meltwater
426 reservoirs existed over seasonal timescales and episodically released large volumes of meltwater able to carve networks like
SG1 and SG2. Finally, it is interesting to note that prolonged surface meltwater ponding in polar desert climates has been
428 associated with changes in regional climate (Stokes et al., 2019). This raises the interesting possibility that the formation of
SG1 and SG2 may record major changes in climate leading to the deglaciation of the IIS.

430 **5 Conclusions**

The subglacial channel networks SG1 and SG2 on Devon Island are consistent with the current set of criteria to identify
432 subglacial channels (e.g., Grau Galofre et al., 2018; Greenwood et al., 2007; Kehew et al., 2012; Sugden et al., 1991): flat-
bottomed cross-sections are common, undulations are present in longitudinal profiles, and tributary channels drain into a
434 larger main stem channel (Fig. 3). We propose that SG1 and SG2 were formed by supraglacial meltwater that reached the
Innuitian Ice Sheet bed via moulins or crevasses (Fig. 6). We do not rule out the subglacial flood hypothesis, however this
436 interpretation provides an alternative meltwater source for cold- to polythermal-based glaciers typically characterized by low



amounts of basal meltwater generation. The planform morphology of these networks, specifically the short, straight, and
438 anastomosing character of tributary channels (Fig. 3A), indicates development during short-lived, episodic events that
occurred at some point during the existence of the Innuitian Ice Sheet.

440 For the first time, fluvial scaling relationships were interrogated for a subglacial system to discuss their hydrology, and to
establish a comparative with river systems. The channel geometry and basin hydrology scaling relationships analysed here
442 (Fig. 5) display distinct differences from the fluvial literature and offer a novel method of distinguishing and characterizing
subglacial meltwater channels, and their water sources, using remote sensing data. A strongly correlated relationship
444 between discharge (channel cross-section area) and channel width emphasizes vertical incision by meltwater rather than
downstream channel widening typical of rivers. Where fluvial systems display a strong relationship between the size of the
446 drainage area and discharge, SG1 and SG2 display a weak relationship that indicates meltwater input from point sources
rather than the catchment-style water input of a fluvial system. This relationship also highlights the influence of other
448 controls on the subglacial meltwater drainage system, such as major climate changes during periods of deglaciation. More
detailed analyses of other networks on Devon Island and other subglacial systems will assist in elucidating these
450 relationships further and may be a useful application to analogue studies of remote environments or other planetary bodies.

Data availability

452 Data for this project, including width and depth measurements for each channel (.xlsx) and DEMs of SG1 and SG2 (.tif), are
available upon request from the lead author, Simona Ruso (sruso@uwo.ca) and can be found in the PANGAEA Earth and
454 Environmental Science data repository (<https://www.pangaea.de/>).

Acknowledgements

456 Funding was provided by a Canadian Space Agency (CSA) Flights and Fieldwork for the Advancement of Science and
Technology (FAST) grant, and a Natural Sciences and Engineering Research Council of Canada (NSERC) Discovery Grant
458 Northern Supplement to GRO. SR thanks the Northern Scientific Training Program (NSTP) for funding. This research was
also supported by H2020 under the MSCA grant agreement n° 101027900, and the Institut National des Sciences de
460 l'Univers – PNP project EGV E&M. Logistical support from the Polar Continental Shelf Program (NRCan) is gratefully
acknowledged. SR also thanks Dr. Shawn Chartrand (Simon Fraser University) for his helpful insight on fluvial scaling
462 relationships and geomorphology.



Author contributions

464 SR, AGG, and GO devised and discussed project idea and timeline. SR and GO collected drone data and field observations
in 2022. SR compiled and analysed drone data, field notes and photos, and developed DEMs, obtained measurements, and
466 carried out morphometric analyses. Literature review and manuscript writing was carried out by SR. AGG and GO provided
insight and edits throughout manuscript writing.

468 Competing interests

The authors declare that they have no conflict of interest.

470 References

- Atkins, C. B.: Geomorphological evidence of cold-based glacier activity in South Victoria Land, Antarctica, *Geol Soc Spec*
472 *Publ*, 381, 299–318, <https://doi.org/10.1144/SP381.18>, 2013.
- Atkins, C. B. and Dickinson, W. W.: Landscape modification by meltwater channels at margins of cold-based glaciers, *Dry*
474 *Valleys, Antarctica, Boreas*, 36, 47–55, <https://doi.org/10.1111/j.1502-3885.2007.tb01179.x>, 2007.
- Bartholomew, I., Nienow, P., Sole, A., Mair, D., Cowton, T., and King, M. A.: Short-term variability in Greenland Ice Sheet
476 motion forced by time-varying meltwater drainage: Implications for the relationship between subglacial drainage system
behavior and ice velocity, *J Geophys Res Earth Surf*, 117, <https://doi.org/https://doi.org/10.1029/2011JF002220>, 2012.
- 478 Beaud, F., Venditti, J. G., Flowers, G. E., and Koppes, M.: Excavation of subglacial bedrock channels by seasonal meltwater
flow, *Earth Surf Process Landf*, 43, 1960–1972, <https://doi.org/10.1002/esp.4367>, 2018.
- 480 Benn, D. I. and Evans, D. J. A.: *Glaciers and Glaciation*, Edward Arnold, London, 1998.
- Bingham, R. G., Hubbard, A. L., Nienow, P. W., and Sharp, M. J.: An investigation into the mechanisms controlling
482 seasonal speedup events at a High Arctic glacier, *J Geophys Res Earth Surf*, 113, <https://doi.org/10.1029/2007JF000832>,
2008.
- 484 Blake, W.: Studies of glacial history in Arctic Canada. I. Pumice, radiocarbon dates, and differential postglacial uplift in the
eastern Queen Elizabeth Islands I, *Can J Earth Sci*, 7, 634–664, <https://doi.org/10.1139/e70-065>, 1970.
- 486 Boon, S., Burgess, D. O., Koerner, R. M., and Sharp, M. J.: Forty-seven Years of Research on the Devon Island Ice Cap,
Arctic Canada, Arctic, 63, 13–29, 2010.
- 488 Boulton, G. S.: Modern Arctic glaciers as depositional models for former ice sheets, *J Geol Soc London*, 128, 361–393,
<https://doi.org/10.1144/gsjgs.128.4.036>, 1972.
- 490 Clapperton, C. M.: Channels formed by the superimposition of glacial meltwater streams, with special reference to the East
Cheviot Hills, North-East England, *Geografiska Annaler: Series A, Physical Geography*, 50, 207–220,
492 <https://doi.org/10.2307/1793388>, 1968.



- Clark, C. D., Ely, J. C., Greenwood, S. L., Hughes, A. L. C., Meehan, R., Barr, I. D., Bateman, M. D., Bradwell, T., Doole,
494 J., Evans, D. J. A., Jordan, C. J., Monteys, X., Pellicer, X. M., and Sheehy, M.: BRITICE Glacial Map, version 2: a map and
GIS database of glacial landforms of the last British-Irish Ice Sheet, *Boreas*, 47, 11–27, <https://doi.org/10.1111/bor.12273>,
496 2018.
- Clayton, L. and Moran, S. R.: A glacial process-form model, in: *Glacial Geomorphology: A proceedings volume of the Fifth*
498 *Annual Geomorphology Symposia Series*, held at Binghamton New York September 26–28, 1974, 89–119,
https://doi.org/10.1007/978-94-011-6491-7_3, 1974.
- 500 Cowton, T., Nienow, P., Bartholomew, I., Sole, A., and Mair, D.: Rapid erosion beneath the Greenland ice sheet, *Geology*,
40, 343–346, <https://doi.org/10.1130/G32687.1>, 2012.
- 502 Cuffey, K. M. and Paterson, W. S. B.: *The physics of glaciers*, Academic Press, 2010.
- Cuffey, K. M., Conway, H., Gades, A. M., Hallet, B., Lorrain, R., Severinghaus, J. P., Steig, E. J., Vaughn, B., and White, J.
504 W. C.: Entrainment at cold glacier beds, *Geology*, 28, 351–354, [https://doi.org/10.1130/0091-7613\(2000\)28<351:EACGB>2.0.CO;2](https://doi.org/10.1130/0091-7613(2000)28<351:EACGB>2.0.CO;2), 2000.
- 506 Das, S. B., Joughin, I., Behn, M. D., Howat, I. M., King, M. A., Lizarralde, D., and Bhatia, M. P.: Fracture propagation to
the base of the Greenland Ice Sheet during supraglacial lake drainage, *Science* (1979), 320, 778–781,
508 <https://doi.org/10.1126/science.115336>, 2008.
- Dewald, N., Livingstone, S. J., and Clark, C. D.: Subglacial meltwater routes of the Fennoscandian Ice Sheet, *J Maps*, 18,
510 382–396, <https://doi.org/10.1080/17445647.2022.2071648>, 2022.
- Dodov, B. and Fofoula-Georgiou, E.: Generalized hydraulic geometry: Insights based on fluvial instability analysis and a
512 physical model, *Water Resour Res*, 40, <https://doi.org/10.1029/2004WR003196>, 2004.
- Dowdeswell, J. A., Benham, T. J., Gorman, M. R., Burgess, D., and Sharp, M. J.: Form and flow of the Devon Island Ice
514 Cap, *Canadian Arctic*, *J Geophys Res*, 109, <https://doi.org/10.1029/2003JF000095>, 2004.
- Dyke, A. S.: Glacial and sea level history of Lowther and Griffith Islands, Northwest Territories: A hint of tectonics,
516 *Géographie Physique et quaternaire*, 47, 133–145, <https://doi.org/10.7202/032944ar>, 1993.
- Dyke, A. S.: Last Glacial Maximum and deglaciation of devon island, arctic canada: support for an inuitian ice sheet,
518 *Quaternary Science Reviews*, 393–420 pp., [https://doi.org/10.1016/S0277-3791\(98\)00005-5](https://doi.org/10.1016/S0277-3791(98)00005-5), 1999.
- Dyke, A. S., Andrews, J. T., Clark, P. U., England, J. H., Miller, G. H., Shaw, J., and Veillette, J. J.: The Laurentide and
520 Inuitian ice sheets during the Last Glacial Maximum, *Quaternary Science Reviews*, 9–31 pp.,
[https://doi.org/10.1016/S0277-3791\(01\)00095-6](https://doi.org/10.1016/S0277-3791(01)00095-6), 2002.
- 522 England, J.: Late Quaternary glaciation of the Eastern Queen Elizabeth Islands, N.W.T., Canada; Alternative models, *Quat*
Res, 6, 185–202, [https://doi.org/10.1016/0033-5894\(76\)90049-1](https://doi.org/10.1016/0033-5894(76)90049-1), 1976.
- 524 England, J.: Support for the Inuitian Ice Sheet in the Canadian High Arctic during the Last Glacial Maximum, *J Quat Sci*,
13, 275–280, [https://doi.org/10.1002/\(SICI\)1099-1417\(199805/06\)13:3<275::AID-JQS374>3.0.CO;2-N](https://doi.org/10.1002/(SICI)1099-1417(199805/06)13:3<275::AID-JQS374>3.0.CO;2-N), 1998.



- 526 England, J., Sharp, M., Lemmen, D. S., and Bednarski, J.: On the extent and thickness of the Innuitian Ice Sheet: a
postglacial-adjustment approach: Discussion, *Can J Earth Sci*, 28, 1689–1695, <https://doi.org/10.1139/e91-152>, 1991.
- 528 England, J., Atkinson, N., Bednarski, J., Dyke, A. S., Hodgson, D. A., and Ó Cofaigh, C.: The Innuitian Ice Sheet:
configuration, dynamics and chronology, *Quat Sci Rev*, 25, 689–703, <https://doi.org/10.1016/j.quascirev.2005.08.007>, 2006.
- 530 Fitzsimons, S. J., Mcmanus, K. J., Sirota, P., and Lorrain, R. D.: Direct shear tests of materials from a cold glacier:
implications for landform development, *Quaternary International*, 86, 129–137, <https://doi.org/10.1016/S1040->
532 6182(01)00055-6, 2001.
- 534 Glasser, N. F. and Bennett, M. R.: Glacial erosional landforms: origins and significance for palaeoglaciology, *Prog Phys*
Geogr, 28, 43–75, <https://doi.org/10.1191/0309133304ppp401ra>, 2004.
- 536 Glasser, N. F. and Smith, G. H. S.: Glacial meltwater erosion of the Mid-Cheshire Ridge: implications for ice dynamics
during the Late Devensian glaciation of northwest England, *J Quat Sci*, 14, 703–710, <https://doi.org/10.1002>, 1999.
- 538 Gleason, C. J.: Hydraulic geometry of natural rivers: A review and future directions, *Prog Phys Geogr*, 39, 337–360,
<https://doi.org/10.1177/0309133314567584>, 2015.
- 540 Grau Galofre, A., Mark Jellinek, A., Osinski, G. R., Zanetti, M., and Kukko, A.: Subglacial drainage patterns of Devon
Island, Canada: Detailed comparison of rivers and subglacial meltwater channels, *Cryosphere*, 12, 1461–1478,
<https://doi.org/10.5194/tc-12-1461-2018>, 2018.
- 542 Greenwood, S. L., Clark, C. D., and Hughes, A. L. C.: Formalising an inversion methodology for reconstructing ice-sheet
retreat patterns from meltwater channels: Application to the British Ice Sheet, *J Quat Sci*, 22, 637–645,
544 <https://doi.org/10.1002/jqs.1083>, 2007.
- 546 Greenwood, S. L., Clason, C. C., and Jakobsson, M.: Ice-flow and meltwater landform assemblages in the Gulf of Bothnia,
Geological Society, London, Memoirs, 46, 321–324, <https://doi.org/10.1144/m46.163>, 2016.
- 548 Gulley, J. D., Grabiec, M., Martin, J. B., Jania, J., Catania, G., and Glowacki, P.: The effect of discrete recharge by moulins
and heterogeneity in flow-path efficiency at glacier beds on subglacial hydrology, *Journal of Glaciology*, 58, 926–940,
<https://doi.org/10.3189/2012JoG11J189>, 2012.
- 550 Hambrey, M. J. and Fitzsimons, S. J.: Development of sediment–landform associations at cold glacier margins, *Dry Valleys*,
Antarctica, Sedimentology, 57, 857–882, <https://doi.org/10.1111/j.1365-3091.2009.01123.x>, 2010.
- 552 Hogan, K. A., Arnold, N. S., Larter, R. D., Kirkham, J. D., Noormets, R., Ó Cofaigh, C., Golledge, N. R., and Dowdeswell,
J. A.: Subglacial Water Flow Over an Antarctic Palaeo-Ice Stream Bed, *J Geophys Res Earth Surf*, 127, e2021JF006442,
554 <https://doi.org/10.1029/2021JF006442>, 2022.
- 556 Jansen, J. D., Codilean, A. T., Stroeven, A. P., Fabel, D., Hättestrand, C., Kleman, J., Harbor, J. M., Heyman, J., Kubik, P.
W., and Xu, S.: Inner gorges cut by subglacial meltwater during Fennoscandian ice sheet decay, *Nat Commun*, 5, 3815,
558 <https://doi.org/10.1038/ncomms4815>, 2014.



- Jørgensen, F. and Sandersen, P. B. E.: Buried and open tunnel valleys in Denmark-erosion beneath multiple ice sheets, *Quat Sci Rev*, 25, 1339–1363, <https://doi.org/10.1016/j.quascirev.2005.11.006>, 2006.
- Kaplan, M. R., Miller, G. H., and Steig, E. J.: Low-gradient outlet glaciers (ice streams?) drained the Laurentide ice sheet, *Geology*, 29, 343–346, [https://doi.org/10.1130/0091-7613\(2001\)029<0343:LGOGIS>2.0.CO;2](https://doi.org/10.1130/0091-7613(2001)029<0343:LGOGIS>2.0.CO;2), 2001.
- Kehew, A. E., Piotrowski, J. A., and Jørgensen, F.: Tunnel valleys: Concepts and controversies - A review, *Earth Sci Rev*, 113, 33–58, <https://doi.org/10.1016/j.earscirev.2012.02.002>, 2012.
- Kirkham, J. D., Hogan, K. A., Larter, R. D., Arnold, N. S., Nitsche, F. O., Gollidge, N. R., and Dowdeswell, J. A.: Past water flow beneath Pine Island and Thwaites glaciers, west Antarctica, *Cryosphere*, 13, 1959–1981, <https://doi.org/10.5194/tc-13-1959-2019>, 2019.
- Kirkham, J. D., Hogan, K. A., Larter, R. D., Arnold, N. S., Nitsche, F. O., Kuhn, G., Gohl, K., Anderson, J. B., and Dowdeswell, J. A.: Morphometry of bedrock meltwater channels on Antarctic inner continental shelves: Implications for channel development and subglacial hydrology, *Geomorphology*, 370, 107369, <https://doi.org/10.1016/j.geomorph.2020.107369>, 2020.
- Kleman, J.: The Palimpsest Glacial Landscape in Northwestern Sweden. Late Weichselian Deglaciation Landforms and Traces of Older West-Centered Ice Sheets, *Geografiska Annaler. Series A, Physical Geography*, 74, 305–325, <https://doi.org/10.1080/04353676.1992.11880373>, 1992.
- Kleman, J. and Borgström, I.: Reconstruction of palaeo-ice sheets: The use of geomorphological data, *Earth Surf Process Landf*, 21, 893–909, [https://doi.org/10.1002/\(SICI\)1096-9837\(199610\)21:10<893::AID-ESP620>3.0.CO;2-U](https://doi.org/10.1002/(SICI)1096-9837(199610)21:10<893::AID-ESP620>3.0.CO;2-U), 1996.
- Kleman, J., Hättestrand, C., and Clarhäll, A.: Zooming in on frozen-bed patches: scale-dependent controls on Fennoscandian ice sheet basal thermal zonation, *Ann Glaciol*, 28, 189–194, <https://doi.org/10.3189/172756499781821670>, 1999.
- Langley, E. S., Leeson, A. A., Stokes, C. R., and Jamieson, S. S. R.: Seasonal evolution of supraglacial lakes on an East Antarctic outlet glacier, *Geophys Res Lett*, 43, 8563–8571, <https://doi.org/10.1002/2016GL069511>, 2016.
- Larter, R. D., Hogan, K. A., Hillenbrand, C.-D., Smith, J. A., Batchelor, C. L., Cartigny, M., Tate, A. J., Kirkham, J. D., Roseby, Z. A., and Kuhn, G.: Subglacial hydrological control on flow of an Antarctic Peninsula palaeo-ice stream, *Cryosphere*, 13, 1583–1596, <https://doi.org/10.5194/tc-13-1583-2019>, 2019, 2019.
- Lee, K. T., Chen, N.-C., and Gartsman, B. I.: Impact of stream network structure on the transition break of peak flows, *J Hydrol (Amst)*, 367, 283–292, <https://doi.org/10.1016/j.jhydrol.2009.01.021>, 2009.
- Lee, P. and Rice, J. W. Jr.: Small valley networks on Mars: The glacial meltwater channel networks of Devon Island, Nunavut Territory, Arctic Canada, as possible analogs, in: *Fifth International Conference on Mars*, <https://doi.org/20000110394>, 1999.
- Lee, P., Rice, J. W. Jr., Bunch, T. E., Grieve, R. A. F., McKay, C. P., Schutt, J. W., and Zent, A. P.: Possible analogs for small valleys on Mars at the Haughton Impact Crater site, Devon Island, Canadian High Arctic, in: *Lunar and Planetary Science Conference*, <https://doi.org/20000092052>, 1999.



- 592 Leopold, L. B. and Maddock, T.: The hydraulic geometry of stream channels and some physiographic implications, US
Government Printing Office, 1953.
- 594 Lewington, E. L. M., Livingstone, S. J., Clark, C. D., Sole, A. J., and Storrar, R. D.: A model for interaction between
conduits and surrounding hydraulically connected distributed drainage based on geomorphological evidence from Keewatin,
596 Canada, *Cryosphere*, 14, 2949–2976, 2020.
- Lewis, A. R., Marchant, D. R., Kowalewski, D. E., Baldwin, S. L., and Webb, L. E.: The age and origin of the Labyrinth,
598 western Dry Valleys, Antarctica: Evidence for extensive middle Miocene subglacial floods and freshwater discharge to the
Southern Ocean, *Geology*, 34, 513–516, <https://doi.org/10.1130/G22145.1>, 2006.
- 600 Livingstone, S. J. and Clark, C. D.: Morphological properties of tunnel valleys of the southern sector of the Laurentide Ice
Sheet and implications for their formation, *Earth Surface Dynamics*, 4, 567–589, <https://doi.org/10.5194/esurf-4-567-2016>,
602 2016.
- Makaske, B.: Anastomosing rivers: a review of their classification, origin and sedimentary products, *Earth Sci Rev*, 53, 149–
604 196, [https://doi.org/10.1016/S0012-8252\(00\)00038-6](https://doi.org/10.1016/S0012-8252(00)00038-6), 2001.
- Mangerud, J. and Berglund, B. E.: The subdivision of the Quaternary of Norden: a discussion, *Boreas*, 7, 179–181,
606 <https://doi.org/10.1111/j.1502-3885.1978.tb00275.x>, 1978.
- Marren, P. M. and Toomath, S. C.: Channel pattern of proglacial rivers: topographic forcing due to glacier retreat, *Earth Surf
608 Process Landf*, 39, 943–951, 2014.
- Nye, J. F.: Water flow in glaciers: jokulhlaups, tunnels and veins, *Journal of Glaciology*, 17, 181–207,
610 <https://doi.org/10.3189/S002214300001354X>, 1976.
- O Cofaigh, C., Lemmen, D. S., Evans, D. J. A., and Bednarski, J.: Glacial landform sediment assemblages in the Canadian
612 High Arctic and their implications for late Quaternary glaciation, *Ann Glaciol*, 28, 195–201,
<https://doi.org/10.3189/172756499781821760>, 1999.
- 614 Osinski, G. R., Lee, P., Spray, J. G., Parnell, J., Lim, D. S. S., Bunch, T. E., Cockell, C. S., and Glass, B.: Geological
overview and cratering model for the Haughton impact structure, Devon Island, Canadian High Arctic, *Meteorit Planet Sci*,
616 40, 1759–1776, <https://doi.org/10.1111/j.1945-5100.2005.tb00145.x>, 2005.
- Price, R. J.: Glacial meltwater channels in the upper Tweed drainage basin, *Geogr J*, 126, 483–489, 1960.
- 618 Rothlisberger, H.: Water pressure in intra- and subglacial channels, *Journal of Glaciology*, 11, 177–203,
<https://doi.org/10.3189/S0022143000022188>, 1972.
- 620 Schoof, C.: Ice-sheet acceleration driven by melt supply variability, *Nature*, 468, 803–806,
<https://doi.org/10.1038/nature09618>, 2010.
- 622 Schumm, S. A., Erskine, W. D., and Tilleard, J. W.: Morphology, hydrology, and evolution of the anastomosing Ovens and
King Rivers, Victoria, Australia, *Geol Soc Am Bull*, 108, 1212–1224, [https://doi.org/10.1130/0016-
7606\(1996\)108<1212:MHAEOT>2.3.CO;2](https://doi.org/10.1130/0016-
624 7606(1996)108<1212:MHAEOT>2.3.CO;2), 1996.



- Schytt, V.: Lateral drainage channels along the northern side of the Moltke Glacier, Northwest Greenland, *Geografiska Annaler*, 38, 64–77, <https://doi.org/10.1080/20014422.1956.11880883>, 1956.
- Shreve, R. L.: Movement of water in glaciers, *Journal of Glaciology*, 11, 205–214, <https://doi.org/10.3189/S002214300002219X>, 1972.
- Simkins, L. M., Greenwood, S. L., Munevar Garcia, S., Eareckson, E. A., Anderson, J. B., and Prothro, L. O.: Topographic controls on channelized meltwater in the subglacial environment, *Geophys Res Lett*, 48, e2021GL094678, <https://doi.org/10.1029/2021GL094678>, 2021.
- Simon, K.: Improved Glacial Isostatic Adjustment Models for Northern Canada, PhD Thesis, University of Victoria, Victoria, 2004.
- Simon, K. M., James, T. S., and Dyke, A. S.: A new glacial isostatic adjustment model of the Innuitian Ice Sheet, Arctic Canada, *Quat Sci Rev*, 119, 11–21, <https://doi.org/10.1016/j.quascirev.2015.04.007>, 2015.
- Sissons, J. B.: Some aspects of glacial drainage channels in Britain. Part II, *Scott Geogr Mag*, 77, 15–36, <https://doi.org/10.1080/00369226108735817>, 1961.
- Sólyom, P. B.: Effect of limited storm duration on landscape evolution, drainage basin geometry, and hydrograph shapes, *J Geophys Res*, 109, <https://doi.org/10.1029/2003jf000032>, 2004.
- Stokes, C. R., Sanderson, J. E., Miles, B. W. J., Jamieson, S. S. R., and Leeson, A. A.: Widespread distribution of supraglacial lakes around the margin of the East Antarctic Ice Sheet, *Sci Rep*, 9, 13823, <https://doi.org/10.1038/s41598-019-50343-5>, 2019.
- Storrar, R. D., Stokes, C. R., and Evans, D. J. A.: Morphometry and pattern of a large sample (>20,000) of Canadian eskers and implications for subglacial drainage beneath ice sheets, *Quat Sci Rev*, 105, 1–25, <https://doi.org/10.1016/j.quascirev.2014.09.013>, 2014.
- Sugden, D. E., Denton, G. H., and Marchant, D. R.: Subglacial meltwater channel systems and ice sheet overriding, Asgard Range, Antarctica, *Geografiska Annaler, Series A*, 73 A, 109–121, <https://doi.org/10.1080/04353676.1991.11880335>, 1991.
- Thorsteinsson, R. and Mayr, U.: The sedimentary rocks of Devon Island, Canadian arctic archipelago, Supply and Services, 1987.
- Tuckett, P. A., Ely, J. C., Sole, A. J., Livingstone, S. J., Davison, B. J., Melchior van Wessem, J., and Howard, J.: Rapid accelerations of Antarctic Peninsula outlet glaciers driven by surface melt, *Nat Commun*, 10, 4311, <https://doi.org/10.1038/s41467-019-12039-2>, 2019.
- Vatne, G. and Irvine-Fynn, T. D. L.: Morphological dynamics of an englacial channel, *Hydrol Earth Syst Sci*, 20, 2947–2964, <https://doi.org/10.5194/hess-20-2947-2016>, 2016.
- Vérité, J., Ravier, É., Bourgeois, O., Bessin, P., Livingstone, S. J., Clark, C. D., Pochat, S., and Mourgues, R.: Formation of murtoos by repeated flooding of ribbed bedforms along subglacial meltwater corridors, *Geomorphology*, 408, 108248, <https://doi.org/10.1016/j.geomorph.2022.108248>, 2022.



- 658 Vérité, J., Ravier, É., Bourgeois, O., Bessin, P., and Pochat, S.: New metrics reveal the evolutionary continuum behind the morphological diversity of subglacial bedforms, *Geomorphology*, 427, 108627, <https://doi.org/10.2139/ssrn.3978870>, 2023.
- 660 Vérité, J., Ravier, É., Bourgeois, O., Pochat, S., and Bessin, P.: The kinematic significance of subglacial bedforms and their use in palaeo-glaciological reconstructions, *Earth Planet Sci Lett*, 626, 118510, <https://doi.org/10.1016/j.epsl.2023.118510>,
662 2024.
- Whipple, K. X. and Tucker, G. E.: Dynamics of stream-power river incision model: Implications for height limits of
664 mountain ranges, landscape response timescales, and research needs, *J Geophys Res*, 104, 17661–17674,
<https://doi.org/10.1029/1999JB900120>, 1999.
- 666 Williams, R. M. E. and Phillips, R. J.: Morphometric measurements of Martian valley networks from Mars Orbiter Laser
Altimeter (MOLA) data, *J Geophys Res Planets*, 106, 23737–23751, 2001.
- 668 Wright, M., Venditti, J. G., Li, T., Hurson, M., Chartrand, S., Rennie, C., and Church, M.: Covariation in width and depth in
bedrock rivers, *Earth Surf Process Landf*, 47, 1570–1582, <https://doi.org/10.1002/esp.5335>, 2022.
- 670 Wyatt, F. R. and Sharp, M. J.: Linking surface hydrology to flow regimes and patterns of velocity variability on Devon Ice
Cap, Nunavut, *Journal of Glaciology*, 61, 387–399, <https://doi.org/10.3189/2015JoG14J109>, 2015.
- 672 Zwally, H. J., Abdalati, W., Herring, T., Larson, K., Saba, J., and Steffen, K.: Surface melt-induced acceleration of
Greenland ice-sheet flow, *Science* (1979), 297, 218–222, <https://doi.org/10.1126/science.1072708>, 2002.